

Segmentation along Strike-Slip Faults Revisited

GHISLAIN DE JOUSSINEAU^{1,2} and ATILLA AYDIN¹

Abstract—Fault segmentation and fault steps and their evolution are relevant to the dynamics and size of earthquake ruptures, the distribution of fault damage zones and the capacity of fault seal. Furthermore, segment interactions and coalescence are the fundamental processes for fault growth. To contribute to this end, we investigated the architecture of strike-slip faults by combining field observations in the Valley of Fire State Park, Nevada, and the published data sets.

First, we studied the trace complexity for 49 faults with offsets ranging from 12 m to 460 km. We established that the number of fault steps (hence fault segments) per unit length is correlated to the maximum fault offset by a negative power law. The faults have longer segments and fewer steps when their offsets increase, indicating the progressive growth, smoothening and simplification of the fault traces as a function of the offset, as proposed by previous investigators.

Second, we studied the dimensions of the segments and steps composing ~ 20 of the previous fault systems. The mean segment length, mean step length and mean step width are all correlated to the maximum fault offset by positive power laws over four orders of magnitude of the offset. In addition, the segment length distributions of four of the faults with offsets ranging from 80 m to 100 km are all lognormal, with most of the segment lengths falling in the range of one to five times the maximum offset of the faults. Finally, the fault steps have an approximately constant length-to-width ratio indicating that, regardless of their environment, strike-slip faults have a remarkable self-similar architecture probably due to the mechanical processes responsible for fault growth. Our data sets can be used as tools to better predict the geometrical attributes of strike-slip fault systems with important consequences for earthquake ruptures, the distribution and properties of fault damage zones, and fault sealing potential.

Key words: Strike-slip faults, fault trace complexity, fault step, fault segment length, fault step length, fault step width, hierarchical self-similar fault architecture.

1. Introduction

Strike-slip faults typically have a complex architecture with numerous segments of various lengths separated by steps (relay zones) of a broad range of sizes. This segmented character of strike-slip fault traces has a direct impact on the dynamics and size of earthquake ruptures, which are believed to initiate generally at small steps (asperities, i.e., features temporarily opposing slip) and terminate at large steps (barriers, i.e., features

¹ Rock Fracture Project, Department of Geological and Environmental Sciences, Stanford University, 450 Serra Mall, Building 320, Stanford, CA 94305, USA.

² Beicip-Franlab, 232 Avenue Napoléon Bonaparte, 92502 Rueil-Malmaison Cedex, France.
E-mail: ghislain.dejousseineau@beicip.com

permanently resisting slip) (SEGALL and POLLARD, 1980; SIBSON, 1985, 1986; BARKA and KADINSKY-CADE, 1988; AKI, 1989; HARRIS *et al.*, 1991; HARRIS and DAY, 1999; OTSUKI and DILOV, 2005; WESNOUSKY, 2006; SHAW and DIETERICH, 2007). Specifically, it has been proposed that the probability of earthquake ruptures to jump from one fault segment to the next decreases exponentially with stepover distance (SHAW and DIETERICH, 2007) and that, in the absence of any linking structure between fault segments, strike-slip fault steps wider than 3–5 km systematically arrest seismic ruptures (HARRIS *et al.*, 1991; WESNOUSKY, 2006). However, further improvement in the comprehension of dynamic rupture along, and fluid flow across, faults requires a sound knowledge of fault discontinuities and their spatial distribution as a function of fault size or slip.

The segmentation of strike-slip fault systems also plays a critical role in controlling the location, orientation and length of fault splays (SEGALL and POLLARD, 1980; DE JOUSSINEAU *et al.*, 2007). These splays, in turn, impact the distribution of damage and the geometrical and statistical properties of secondary fault networks around strike-slip faults (FLODIN and AYDIN, 2004; MYERS and AYDIN, 2004; DE JOUSSINEAU and AYDIN, 2007). Moreover, the fault architecture affects the repartition of slip and stress along fault systems, with important consequences for damage zone distribution (CARTWRIGHT *et al.*, 1995; KNOTT *et al.*, 1996; DE JOUSSINEAU and AYDIN, 2007; FINZI *et al.*, 2009). Finally, fault segmentation controls the development of fault core that forms preferentially in stepovers because of high strain levels therein. This is critical for fluid flow in the subsurface since damage zones typically have higher permeability than the parent rock whereas fault cores usually have lower permeability (CAINE *et al.*, 1996; JOURDE *et al.*, 2002; AYDIN, 2000; ODLING *et al.*, 2004).

Notwithstanding its importance, the architecture of strike-slip faults in the subsurface cannot easily be detected accurately by seismic techniques which typically identify faults as line elements and fail to separate closely-spaced segments. Consequently, attempts to better predict the geometrical features of strike-slip faults have been made. Based on the analysis of strike-slip fault traces, WESNOUSKY (1988) and STIRLING *et al.* (1996) found that the number of fault steps (hence fault segments) per unit length is a decreasing function of the maximum fault offset. This structural evolution by which strike-slip fault traces smoothen and straighten progressively with increasing offset is expected to impact the seismological behavior of faults (WESNOUSKY, 1988; SCHOLZ, 2002; BEN-ZION and SAMMIS, 2003) as well as the distribution of fault damage zones (DE JOUSSINEAU and AYDIN, 2007). However, due to the lack of data for the entire spectrum of fault size, it is still unclear whether the relationship between strike-slip fault trace complexity and fault offset hold true in all situations.

From a different angle, AYDIN and NUR (1982) analyzed the shape of fault steps along major strike-slip faults and showed that the length to width ratio of these steps was more-or-less constant. Based on this finding, they proposed conceptual models for the structural evolution of strike-slip fault systems, in which the coalescence of neighboring basins and/or the formation of new fault strands parallel to the existing ones account for the progressive enlargement of fault steps with increasing offset.

From an experimental point of view, OTSUKI and DILOV (2005) determined that strike-slip faults developing in rock samples subjected to cyclic loading had a hierarchical self-similar architecture. At each stage of the fault evolution, the segments were composed of smaller segments and steps related to earlier stages of fault evolution, and the fault length was correlated to the mean segment length, mean step length and mean step width by positive power laws. This hierarchical self-similar architecture of strike-slip faults is expected to strongly impact the nucleation and termination of earthquake ruptures. However, to our knowledge, no comparable data set is available from natural faults, thus making it uncertain whether the results of these experiments are applicable to geological situations.

In this paper, we combine field studies of strike-slip fault zones, published data sets and analyses of published fault maps to develop a basis for a better understanding and forecasting of the architecture of strike-slip faults. First, we confirm the existence of a negative power law relationship between the number of steps per unit length and the maximum fault offset over five orders of magnitude of the offset. Second, we show that the mean segment length is correlated to the maximum fault offset by a positive power law. We also analyze the segment length distribution in a series of faults and observe common features between the distributions independently of the fault offset. Finally, we establish that there is a positive power law relationship between the mean step length and mean step width and the maximum fault offset, and confirm that the length to width ratio of strike-slip fault steps falls into a narrow range.

This work provides additional data for the remarkable self-similarity of the architecture of strike-slip faults, and forms a basis for an improved understanding of strike-slip fault characteristics. In turn, these results have critical implications for the dynamics of seismic ruptures, fault growth processes, the distribution and properties of fault damage zones and fault sealing capacity.

2. *Methods*

In this paper, we follow AYDIN and NUR (1982) and WESNOSKY (1988) and use the term 'step' to refer to the relay zones between the segments along strike-slip faults (regardless of their extensional or compressive nature). We present data on the architecture of a fairly large population of strike-slip faults obtained from our own field study, data sets published by other workers and analyses of fault maps in the literature. The new field data were collected in the Valley of Fire State Park, located approximately 60 miles NE of Las Vegas in southeastern Nevada (Fig. 1a). In this area, excellent outcrops of aeolian Jurassic Aztec Sandstone allow to study of well-exposed strike-slip fault networks at centimeters to kilometers scale. The mechanisms of formation and evolution of these fault networks and their geometrical and statistical properties were previously documented by MYERS and AYDIN (2004), FLODIN and AYDIN (2004) and DE JOUSSINEAU and AYDIN (2007).

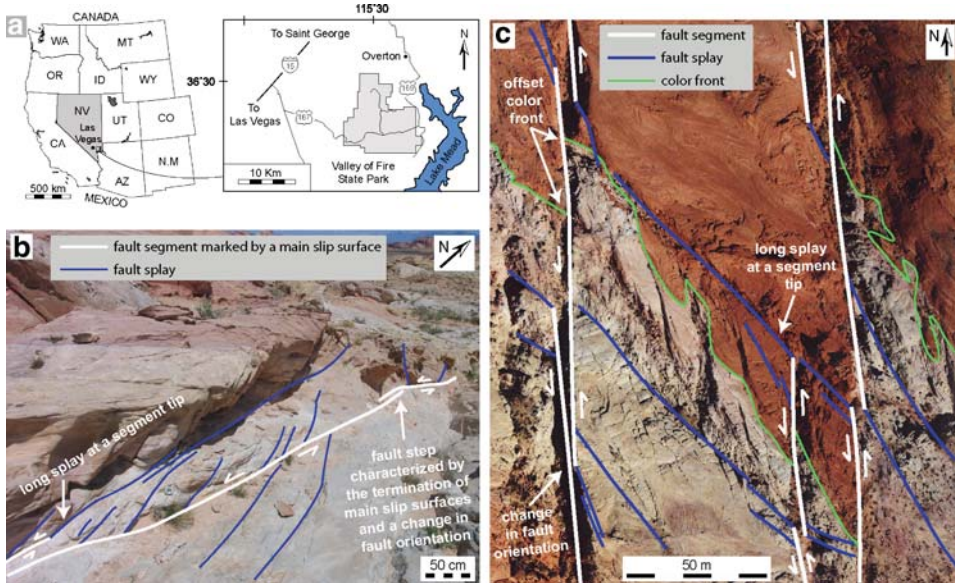


Figure 1

(a) Geographic location of the Valley of Fire State Park, SE Nevada (modified from FLODIN and AYDIN, 2004); (b) Ground photograph showing the architecture of a small fault system (slip ~ 10 m); (c) Aerial photograph showing the architecture of two large fault systems (slip ~ 100 m or more). The tips of fault segments are often associated with large splays (b, c). Fault steps are usually characterized by the termination of main slip surfaces (b) and by changes in the general orientation of the fault zone (b, c). Offset color fronts provide an estimate of the amount of lateral slip for large faults (c).

The size and number of segments and steps along a series of faults in the Valley of Fire were first determined on high-quality aerial photographs and were then validated in the field, with a final (field-based) resolution of a few tens of meters for the largest faults studied (offset ≥ 600 m), a few meters for intermediate faults ($14 \text{ m} < \text{offset} < 600$ m) and a few tens of centimeters for the smallest faults studied (offset ≤ 14 m). Criteria used to decipher the fault segmentation in the field were the morphology and orientation of the fault zones, the continuity of slip surfaces, the continuity and thickness variations of fault core and fault damage zone and the location of main splays along the faults that may indicate the tips of large segments (DE JOUSSINEAU *et al.*, 2007) (Figs. 1b and 1c). The maximum separation on map view was considered as the maximum fault offset, that is faults are assumed to be pure strike-slip. For small faults (with ~ 10 m of offset), the maximum fault offset was determined in the field based on the displacement of markers such as dune boundaries or color bands inherited from diagenetic processes (EICHHUBL *et al.*, 2004) or other structural markers like older shear bands and compaction bands. For intermediate or large faults (with ~ 100 m of offset or more), the maximum fault offset was determined on aerial photographs based on the displacement of major chemical reaction fronts marking the limit between different diagenetic units appearing in various

colors in the Aztec Sandstone (EICHHUBL *et al.*, 2004; Fig. 1c). These offsets were also field-checked afterwards.

We used the published data from WESNOUSKY (1988) and STIRLING *et al.* (1996) together with new data obtained from analyses of published fault maps. The fault examples selected in the literature were those for which detailed maps were available and the maximum fault offsets were known. These examples come from sedimentary, metamorphic and volcanic environments, making the results of the study applicable to a wide range of settings.

For each fault example, the dimensions of segments and steps were measured directly on the fault maps. The number of steps per unit length (km) was obtained by dividing the number of steps by the length (in km) over which the faults were analyzed. The mean values of the segment length, step width and step length are arithmetic average values. For the steps, the configurations of both overlapping and underlapping steps were considered. The imprecision in the data is shown in the plots by error bars where applicable. It is related either to determination of the maximum fault offset, the number of steps per kilometer (i.e., the number of segments composing the fault systems) or both, and was estimated by the authors of the original studies.

Finally, certain studies provided intervals of values instead of exact values for the maximum fault offset or the number of steps per km, making it difficult to plot the data. In this case, we calculated an arithmetic average value for the parameter considered, assigned it to the fault studied, and considered the imprecision in the estimation of the parameter to be the difference between this average value and the lower and upper boundaries of the interval. For example, if a fault offset was reported to be in the interval 1–5 km, we considered that the fault offset was 3 ± 2 km.

3. Results

3.1. Fault Trace Characterization

Here we examine the trace complexity of a series of strike-slip faults in the field in the Valley of Fire State Park and in the literature to complement the data sets in WESNOUSKY (1988) and STIRLING *et al.* (1996). Figure 2 shows plots of the number of steps per km as a function of the maximum strike-slip offset for 49 faults with offsets ranging from 12 m to 460 km, with the source of the data indicated. Data in Figure 2 (also given in Table 1) are best fit by a negative power law relationship: $y = 0.26x^{-0.81}/R^2 = 0.74$, where the number of steps and the maximum offset are plotted on y and x axis, respectively. In addition, best fits to the data from the Valley of Fire, data of STIRLING *et al.* (1996) and data of WESNOUSKY (1988) are given and discussed in Section 4.1. Confidence intervals calculated for the mean and single values of the number of steps with a confidence threshold of 95% are also represented, as in all following comparable figures. The best-fit relationship determined over a large range of data in Figure 2 indicates that the strike-slip faults considered here for

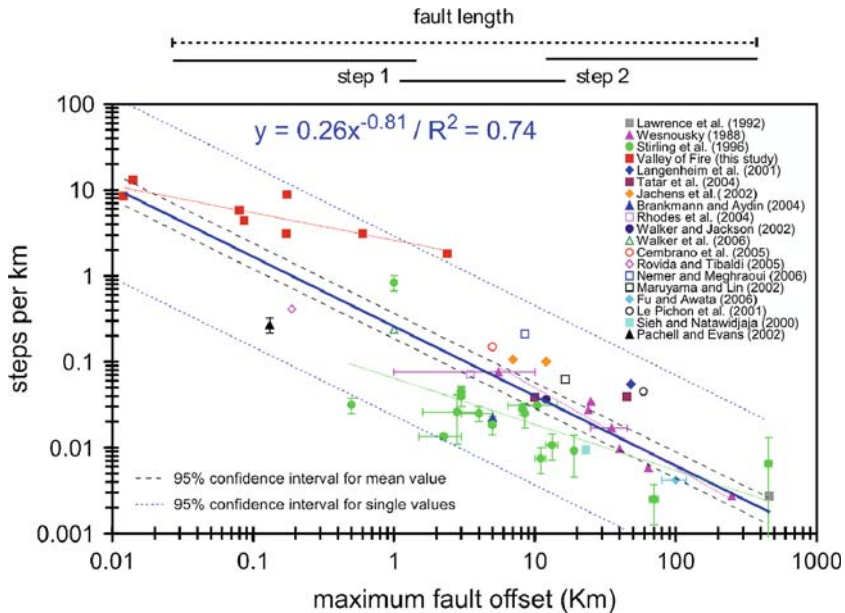


Figure 2

Relationships between the maximum fault offset and the number of steps per km for the strike-slip faults from this study and the published literature as referenced on the figure. The best (power) fits to the general data (solid blue line) and to individual data (Valley of Fire: dotted red line; STIRLING *et al.*, 1996: dotted green line; WESNOUSKY, 1988: dotted pink line) are given. The (95%) confidence intervals for the mean (dashed black lines) and single (dashed blue lines) values of the number of steps per km are also shown.

the statistical analyses have longer segments and fewer steps with increasing slip magnitudes, which is related to the fundamental process of fault growth by segment coalescence (CARTWRIGHT *et al.*, 1995; DE JOUSSINEAU and AYDIN, 2007). These results extend and confirm those from previous studies (WESNOUSKY, 1988; STIRLING *et al.*, 1996).

3.2. Segment Length

Here we consider the segment length in ~ 20 of the faults in Figure 2, for which segments and their tips and steps could be identified so that adequate mean segment lengths, mean step lengths and mean step widths (see Section 3.3) could be measured. Figure 3 shows a clear positive power law relationship between the mean segment length and the maximum fault offset: $y = 2.16x^{0.89} / R^2 = 0.87$, where the mean segment length and the maximum offset are plotted on y and x axis, respectively. Results in Figure 3 are consistent with those in the experimental study by OTSUKI and DILOV (2005). In their study, the data were plotted against fault length instead of fault offset as in our work. However, as these two fault parameters are thought to be correlated (COWIE and SCHOLTZ,

Table 1

Data plotted in Figure 2. *Note that also a value of 65 km was proposed in the literature

Source study	Fault name	Scale	Max. fault offset (km)	Number of steps per km
This study	Classic	1/3800	0.175	8.9
	12 m	1/1000	0.012	8.5
	86 m	1/3800	0.086	4.4
	172 m	1/3800	0.172	3.1
	Lonewolf	1/3800	0.08	5.78
	14 m	1/1000	0.014	13.1
	Baseline Mesa	1/37000	2.4	1.81
	600 m	1/37000	0.6	3.09
WESNOUSKY (1988)	Newport-Ingelwood	1/1050000	5.5 ± 4.5	0.0758
	Calaveras-Green Valley	1/345000	24	0.0275
	San Jacinto	1/323000	25	0.0345
	Whittier-Elsinore	1/4000000	40	0.00965
	Garlock	1/3030000	64	0.00585
	San Andreas	1/2940000	250	0.00275
	North Anatolian	1/4550000 to 1/2850000	35 ± 10*	0.017
STIRLING <i>et al.</i> (1996)	Helendale	1/530000	3	0.045 ± 0.007
	Calico-Mesquite	1/870000	8.2	0.028 ± 0.004
	Pisgah	1/500000	10.4 ± 4	0.031
	Camp Rock	1/570000	2.8 ± 1.2	0.026 ± 0.015
	Lenwood	1/480000	2.25 ± 0.75	0.0135 ± 0.0005
	San Miguel-Vallecitos	1/1090000	0.5	0.0315 ± 0.0065
	MTL (Shikoku island)	1/1330000	5	0.0185 ± 0.0045
	Neodani	1/670000	4 ± 1	0.025 ± 0.005
	Atera	1/600000	8.5 ± 1.5	0.025 ± 0.008
	Atotsugawa	1/590000	3	0.040 ± 0.01
	Tanna	1/310000	1	0.835 ± 0.165
	Wairau	1/550000	455 ± 25	0.0065 ± 0.0065
	Hope	1/1560000	19	0.00925 ± 0.00473
	Wellington	1/1820000	11 ± 1	0.0075 ± 0.0025
	Altun	1/5000000	70 ± 5	0.0025 ± 0.00125
Haiyuan	1/1670000	13.25 ± 1.25	0.01072 ± 0.00358	
LAWRENCE <i>et al.</i> (1992)	Chaman Transform Zone	1/2500000	460	0.00273
LANGENHEIM <i>et al.</i> (2001)	Las Vegas Valley Shear Zone (North trend)	1/1030000	48	0.0549
	TATAR <i>et al.</i> (2004)	Amanos	1/800000	45
JACHENS <i>et al.</i> (2002)	East Hatay	1/800000	10	0.03825
	Ludlow	1/1750000	12	0.1
BRANKMAN and AYDIN (2004)	Blackwater	1/1750000	7	0.10638
	Mattinata	1/510000	5	0.02234
RHODES <i>et al.</i> (2004)	Mae Kuang	1/360000	3.5	0.07143
WALKER and JACKSON (2002)	Gowk	1/9500000	12	0.03659
WALKER <i>et al.</i> (2006)	Jid	1/230000	1	0.23684
CEMBRANO <i>et al.</i> (2005)	Coloso	1/180000	5	0.14865
ROVIDA and TIBALDI (2005)	Buesaco	1/77000	0.188	0.4116
NEMER and MEGHRAOUI (2006)	Roum	1/180000	8.5	0.211

Table 1

contd.

Source study	Fault name	Scale	Max. fault offset (km)	Number of steps per km
MARUYAMA and LIN (2002)	Arima-Takatsuki Tectonic Line	1/440000	16.5	0.0625
FU and AWATA (2006)	Kunlun	1/10000000	100 ± 20	0.00422
LE PICHON <i>et al.</i> (2001)	Marmara	1/1300000	59	0.045
SIEH and NATAWIDJAJA (2000)	Great Sumatran	1/4620000	23	0.00947
PACHELL and EVANS (2002)	Gemini	1/62500	0.131	0.2688 ± 0.0538

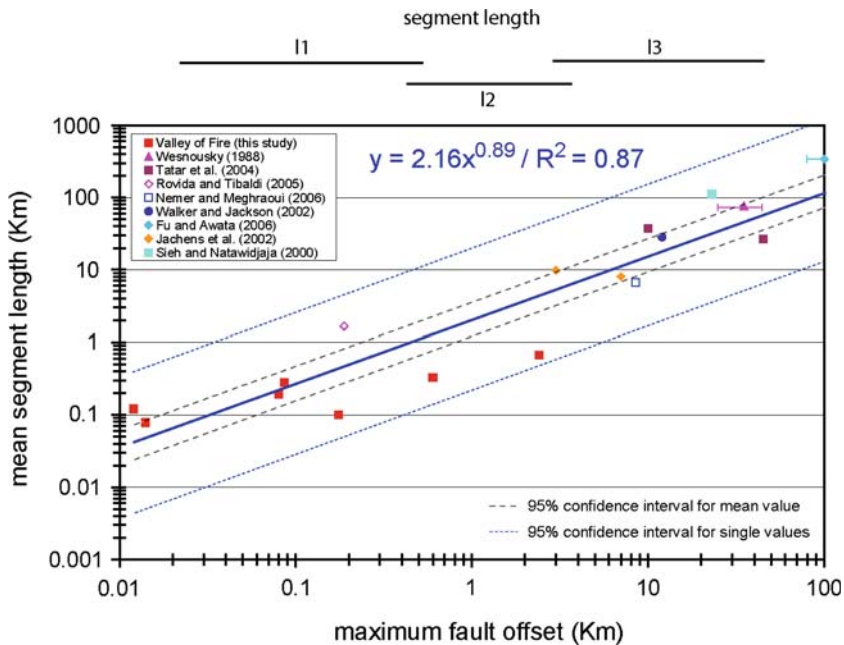


Figure 3

Relationships between the maximum fault offset and the mean segment length for strike-slip faults from this study and the published literature as referenced on the figure. The best (power) fit to the data and the (95%) confidence intervals for the mean and single values of the mean segment length are shown.

1992; DAWERS *et al.*, 1993; SCHLISCHE *et al.*, 1996), direct comparisons could be made between our results and those in OTSUKI and DILOV (2005).

Figure 4 provides additional constraints on strike-slip fault segment lengths by showing segment length distributions for four of the faults in Figure 3 with offsets ranging from 80 m to 100 km. All of these distributions are lognormal. Moreover, for each fault, all of the segments have a length falling in the range of zero to ten times the maximum fault offset ‘d’, with most of the segment lengths in the interval 1d–5d (see data in Table 2).

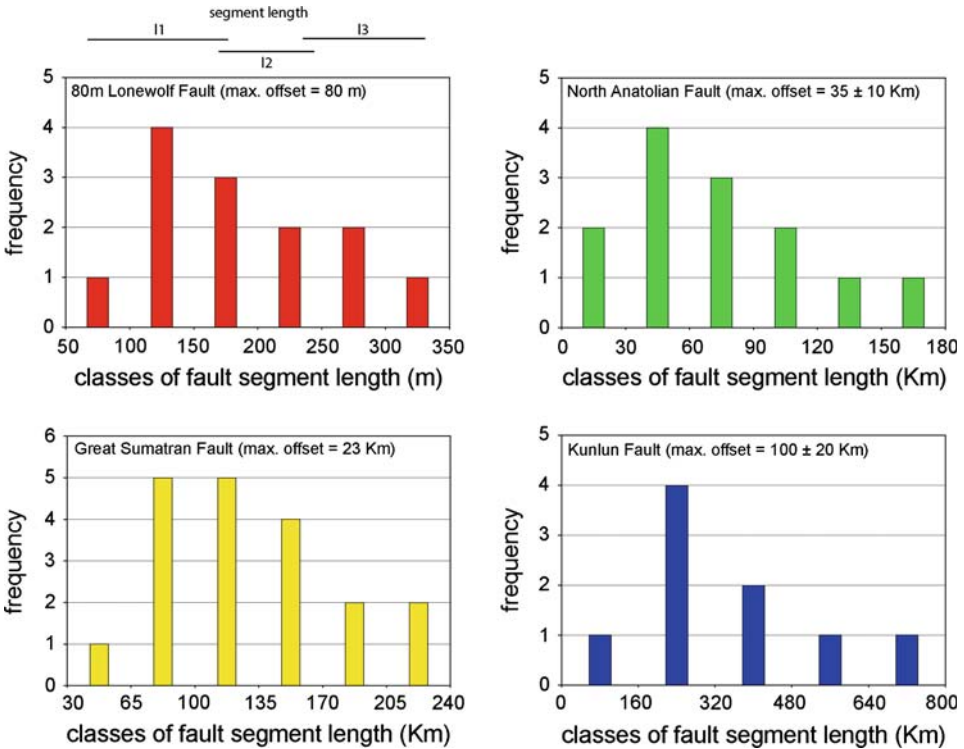


Figure 4 Segment-length frequency distributions for four strike-slip faults. Fault names and offsets are indicated.

3.3. Step Dimensions

We also investigated the mean step length and mean step width in the same faults as in Figure 3, augmented by two new fault examples where enough steps could be measured but insufficient segment length data were available. The data set in Figure 5 presents a clear positive power law relationship between the mean step length and the maximum fault offset: $y = 0.30x^{0.77}/R^2 = 0.84$, where the mean step length and the maximum offset are plotted on y and x axis, respectively. Figure 6 illustrates the same kind of relationship between the mean step width and the maximum fault offset: $y = 0.12x^{0.80}/R^2 = 0.81$, where the mean step width and the maximum offset are plotted on y and x axis, respectively. Again, these results are consistent with those in OTSUKI and DILOV (2005).

Finally, Figure 7 shows the relationships between step width and step length for the faults analyzed in this study and for the faults compiled in AYDIN and NUR (1982). The data of the two sets align very well and are best fit by a quasi-linear positive power law relationship: $y = 2.69x^{0.97}/R^2 = 0.93$, where the step length and step width are plotted on y and x axis, respectively. This relationship is very similar to that in AYDIN and NUR (1982) and indicates that the length-to-width ratio of fault steps falls into a narrow range with an average value of slightly less than 3 (~2.7 for this study).

Table 2

*Data plotted in Figure 4. *Note that also a value of 65 km was proposed in the literature*

Source study	Fault name	Scale	Max. fault offset, d (km)	Segment length (km)	Segment length (d)
This study	Lonewolf	1/3800	0.08	0.079	0.99
				0.102	1.28
				0.129	1.61
				0.139	1.74
				0.149	1.86
				0.188	2.35
				0.191	2.39
				0.191	2.39
				0.201	2.51
				0.234	2.93
				0.271	3.39
				0.274	3.43
				0.347	4.34
				SIEH and NATAWIDJAJA (2000)	Great Sumatran
60	2.61				
60	2.61				
65	2.83				
70	3.04				
70	3.04				
85	3.7				
85	3.7				
90	3.91				
95	4.13				
95	4.13				
120	5.22				
125	5.43				
150	6.52				
150	6.52				
160	6.96				
180	7.83				
200	8.7				
220	9.57				
WESNOUSKY (1988)	North Anatolian	1/4550000 to 1/2850000	35 ± 10 (*)	23	0.65
				27	0.78
				46	1.3
				47	1.35
				59	1.67
				59	1.69
				70	1.99
				77	2.2
				78	2.24
				96	2.73
				102	2.92
				127	3.63
				179	5.12

Table 2

contd.

Source study	Fault name	Scale	Max. fault offset, d (km)	Segment length (km)	Segment length (d)
FU and AWATA (2006)	Kunlun	1/10000000	100 ± 20	135	1.35
				230	2.3
				270	2.7
				300	3
				300	3
				330	3.3
				340	3.4
				480	4.8
				680	6.8

4. Discussion and Implications

4.1. Scale- and Resolution-related Biases

Because this paper aims to analyze the architecture of strike-slip faults over a wide range of magnitude of the fault offset, the data presented in Figures 2 to 7 were obtained from faults of very different sizes that were mapped at different scales, i.e., with different resolutions. These variations in resolution of the mapping, inherent to any compilation work, could possibly introduce a bias in the data sets. In particular, the trends observed in Figures 2, 3, and 5–7 may be affected by the mapping resolution, with the larger faults being mapped with a lesser degree of detail than the smaller ones, i.e., tending to have longer segments and fewer steps. However, there are strong arguments supporting the existence of the trends in the data sets. First, the concept that faults become smoother as they mature is well accepted. In particular, previous studies by WESNOUSKY (1988) and STIRLING *et al.* (1996) have established clear relationships between maximum strike-slip fault offset and strike-slip fault trace complexity over up to three orders of magnitude of the fault offset (offsets ranging from 500 m to 455 km). Our study complements those results and expands them to smaller fault scales (offsets down to 12 m). In addition, the same trends are observed in the data corresponding to the faults from the Valley of Fire. These faults have been mapped with great care and at resolutions that are nearly uniform in a range of scales, so that scale and resolution biases were avoided to the extent possible. The fact that clear relationships between maximum fault offset and number of steps per km, mean segment length, mean step length and mean step width are observed in these data suggests that the trends in the general data sets in Figures 2, 3 and 5–7 have geological and mechanical origins which are likely related to fault growth processes, as discussed in the next section.

Examination of the Valley of Fire data in Figures 2–3 and 5–6 may suggest the existence of trends that are different from the trends in other data sets and the general trends of the combined data. For example, in Figure 2, data from the Valley of Fire may

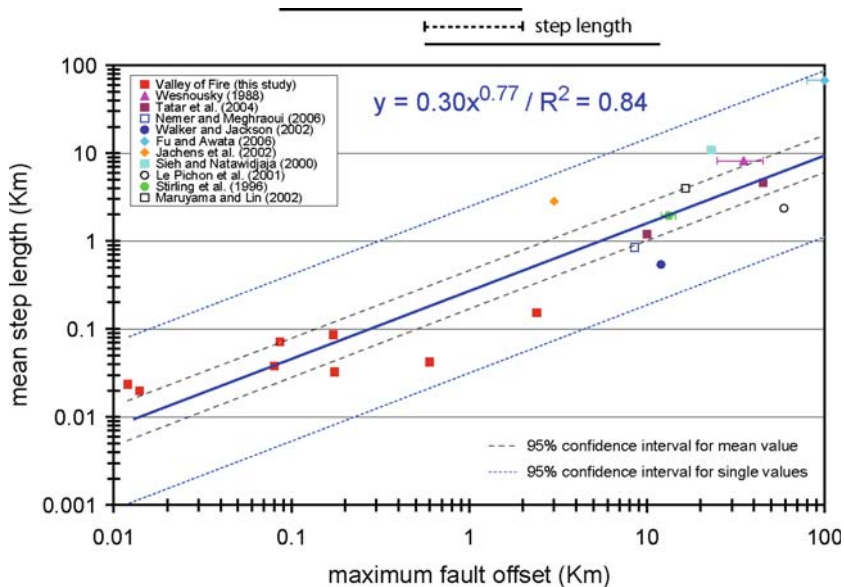


Figure 5

Relationships between the maximum fault offset and the mean step length for strike-slip faults from this study and the published literature as referenced on the figure. The best (power) fit to the data and the (95%) confidence intervals for the mean and single values of the mean step length are shown.

be fit by a power law with an exponent of ~ 0.32 , whereas the power trend for the combined data has an exponent of ~ 0.81 , and power trends fitting the data of STIRLING *et al.* (1996) and WESNOUSKY (1988) have exponents of ~ 0.52 and ~ 0.94 , respectively. This is a very common observation in any combined data set. For example, SCHLISCHE *et al.* (1996) provided a combined data set for the relationships between fault length and maximum fault slip. It is clear in their data set that each particular population of data can be characterized by its own trend that is different from the general trend of the combined data. Similar observations can be made in the data set in DAWERS *et al.* (1993). Such differences in the trends of the different individual data sets were generally attributed, among others, to different rock types and geological contexts or different mechanical behaviors of faulted rocks (DAWERS *et al.*, 1993; SCHLISCHE *et al.*, 1996). They appear to reflect the actual variability that exists in nature.

However, it is also possible that the scaling parameters may change with the size of the structural features and the scale of observation, i.e., that the data could be characterized by different trends at different scale intervals. For the relationships between fault length and maximum fault slip, it has been proposed that there is a characteristic dimension at which scaling parameters change in relation with either a change in the geometry of fault growth or different material properties encountered by faults that propagate into deeper parts of the crust as their sizes increase (DAWERS *et al.*, 1993).

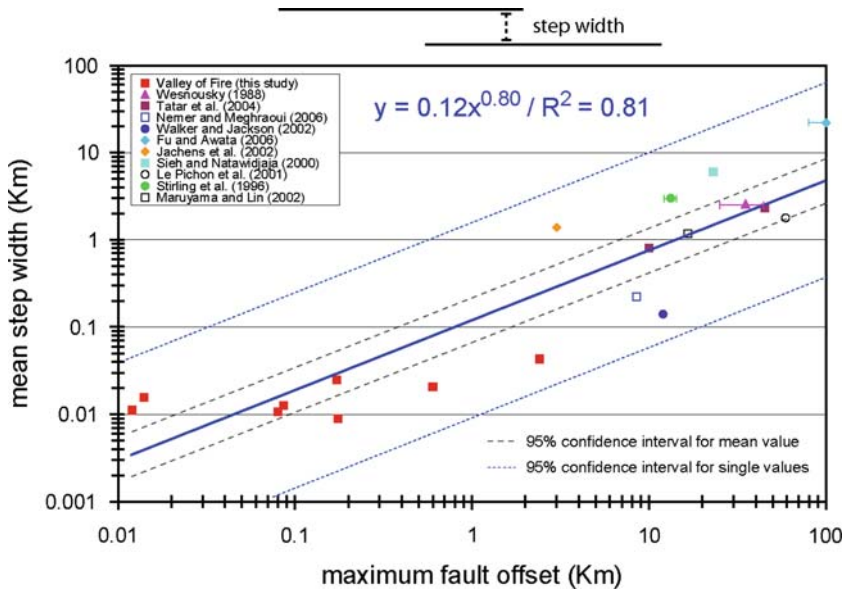


Figure 6

Relationships between the maximum fault offset and the mean step width for strike-slip faults from this study and the published literature as referenced on the figure. The best (power) fit to the data and the (95%) confidence intervals for the mean and single values of the mean step width are shown.

In our study, the different trends in Figure 2 may partly owe their existence to scale differences. The data obtained from faults mapped at a relatively small scale in the Valley of Fire may be skewed towards high numbers of steps per unit length, hence exhibit lower power law exponents than the data obtained from faults mapped at larger scales. Also, the different trends in Figure 2 may indicate a change in scaling parameters with the size of features, in relationship to changes in fault growth processes. However, several observations suggest that this may not be the case. First, no clear change in the scaling parameters for a given value of the fault offset is observed in the data. There is no clear break in the data in Figure 2 but a relative scatter of data at all scales. For instance, data based on the studies by STIRLING *et al.* (1996), PACHELL and EVANS (2002), ROVIDA and TIBALDI (2005) or WALKER *et al.* (2006) plot below the Valley of Fire data for similar strike-slip fault offsets. Second, the trend fitting the data of STIRLING *et al.* (1996) has an exponent that is closer to the one in the Valley of Fire data than to the one in the data of WESNOUSKY (1988), although STIRLING *et al.* (1996) and WESNOUSKY (1988) both studied large-scale faults. This suggests that the different trends in Figure 2 are more related to different contexts and lithologies or different mechanical behaviors of rocks than to changes in scaling relationships with the size of features. It follows that the global trends in Figures 2, 3, 5 and 7 may be more-or-less valid, even if the existence of possible biases due to scale variability in the original fault maps cannot be completely ruled out.

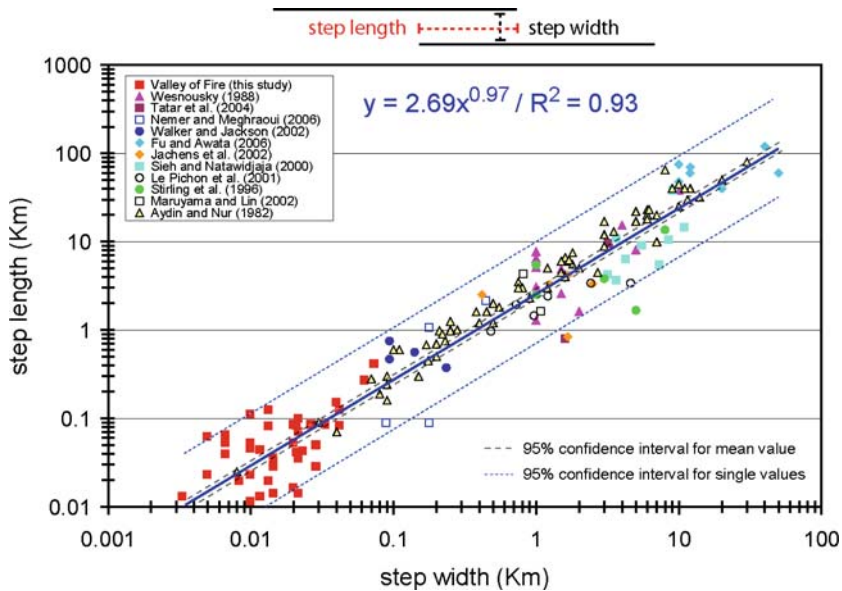


Figure 7

Relationships between step width and step length for strike-slip faults from this study and the published literature as referenced on the figure. The best (nearly-linear power) fit to the data and the (95%) confidence intervals for the mean and single values of the step length are shown.

4.2. Fault Growth and Evolution

It is now widely accepted that brittle faults start from a series of short echelon arrays and grow by linkage of the neighboring segments (SEGALL and POLLARD, 1980; CARTWRIGHT *et al.*, 1995; MYERS and AYDIN, 2004; KIM *et al.*, 2004). It then follows that steps are destructed by through-going planar surfaces to produce more continuous and smoother fault segment geometry at larger scales while new segments achieve a greater capability to interact with each other at a greater distance (AYDIN and SCHULTZ, 1990; SCHOLZ, 2002). BEN-ZION and SAMMIS (2003) characterized this process of fault growth and maturation by summing up that fault structures tend to evolve toward geometric simplicity at all scales. The data related to the size and density distribution of fault steps and the evolution of fault segment length we presented in this paper are consistent with these notions.

It appears that the underlying mechanical principle for many of these phenomena is rather simple. First, for a mode-II fracture, the stress components at a point in the regions away from the fracture tips decay as $(a/r)^2$ for 2-D (POLLARD and SEGALL, 1987) and $(a/r)^3$ for 3-D (BEN-ZION and SAMMIS, 2003), where “a” is the half fault length and “r” is the radial distance to the center of the fault. Second, fault interaction is an important factor in the final fault geometry. AYDIN and SCHULTZ (1990) investigated the influence of fault geometry as well as the sense of step using a 2-D mode-II fracture interaction model.

They concluded that the relative locations of the neighboring fracture tips strongly impact echelon mode-II fracture geometry although this influence is more-or-less independent of the sense of echelon step. They also determined that fault propagation energy first increases as the fault tips approach each other and then decreases sharply as the fracture tips pass by each other. The data on the step size and distribution are consistent with these notions.

Finally, our analyses of strike-slip fault steps complement those in AYDIN and NUR (1982) and confirm that the length-to-width ratio of fault steps is more-or-less constant. This supports the conceptual models of evolution of strike-slip fault systems in which the size of fault steps progressively increases through the coalescence of neighboring relay zones and/or the formation of new fault strands parallel to the existing ones during fault growth.

4.3. *Seismic Rupture*

Our results indicate that the trace complexity of strike-slip faults is a smoothly decreasing function of the fault offset, implying that larger faults have fewer and larger steps and longer segments than smaller faults. This may have important implications for fault growth processes and earthquake ruptures. First, it is explicit evidence for the universality of fault segment linkage and coalescence or the straightening of fault traces by obliteration and/or elimination of steps at certain stages of fault development. Second, strength properties of fault zones partly depend on the presence of fault steps which oppose the slip and act as asperities or barriers for rupture events along the faults (SIBSON, 1986; AKI, 1989). As the distribution of steps along strike-slip faults is a function of the fault offset, it follows that the strength properties of faults may also be partly correlated with the offset. This supports the proposition by WESNOSKY (1988) that strike-slip faults, together with their structural evolution, may undergo a seismological evolution whereby the size and frequency distribution of slip events are a function of the fault offset.

Our results also provide a basis for applying the experimental results of OTSUKI and DİLOV (2005) to natural faults. These authors observed that strike-slip faults developing sequentially in rock samples had a hierarchical self-similar architecture wherein the fault segments of a higher hierarchical rank (i.e., newly developed) were composed of smaller segments and steps of a lower hierarchical rank (i.e., developed during previous stages of fault evolution). In addition, the length of the fault systems was correlated to the mean segment length, mean step length and mean step width by positive power laws. Based on these observations, they derived the Gutenberg-Richter law and the empirical relationship of the length of the seismic nucleation zone to the seismic moment and proposed that the seismic rupture mimics the hierarchical geometry of fault zones, by nucleating at a small step of a lower hierarchical rank and terminating at a large step of higher hierarchical rank. Our analyses of natural strike-slip fault zones yielded results that compare well with those of OTSUKI and DİLOV (2005). This suggests that natural strike-slip faults may have the same hierarchical self-similar architecture as the faults in their experiments. Thus,

their reasoning in terms of the impact of fault architecture on the dynamics of seismic ruptures could also apply to natural geological faults. This idea is also supported by recent conceptual models for the development of strike-slip fault zones (MYERS and AYDIN, 2004; FLODIN and AYDIN, 2004; DE JOUSSINEAU and AYDIN, 2007), which proposed that strike-slip faults have a hierarchical pattern where, at each stage of the fault evolution, the fault segments can be broken into a series of smaller segments and steps related to earlier phases of fault development. It is likely that new, short segments are also generated as faults grow. However, the rate of generation of such short segments along a given mature fault is probably small compared with the rate of development of large segments by coalescence of earlier, shorter segments.

We should, however, note that predicting the distribution and size (length and width) of steps along faults may not be sufficient for forecasting the nucleation site and extent of seismic ruptures. Other important parameters have an effect on fault strength properties and the dynamics of earthquake ruptures. Particularly, ruptures may be influenced by the orientation of fault segments with respect to the regional tectonic stress field. Examples of a rupture jumping across a major fault step because the orientation of the fault segment that was being ruptured was becoming unfavorable have been documented, as in the 1992 Landers earthquake (BOUCHON *et al.*, 1998). However, even if the mechanics of earthquake rupture is complex and its size and location cannot entirely be forecasted by knowing or estimating the pattern and architecture of the related geological faults, this knowledge still provides valuable information regarding one of the important parameters influencing the nucleation and termination of earthquake ruptures.

4.4. Prediction of Subsurface Fault Attributes and Fluid Flow

This study, by establishing the general self-similar architecture of strike-slip faults and the relationships between the maximum fault offset and the dimensions of fault segments and steps, may allow one to better forecast the geometrical attributes of strike-slip faults. This has important implications for the internal structure of fault zones, the distribution of damage zones and the properties of secondary fault networks associated with strike-slip fault systems.

First, it may be possible to estimate the width of steps along a given fault of known length or offset (both being correlated). Steps are locations of the faults where fault rocks and damage zones develop preferentially by progressive fracturing and crushing of the host rock because of high stress concentration therein. Thus, determining the dimensions of fault steps could provide the size of the largest pockets of initially fractured rocks and later fault core along the mature fault zones. This is important in terms of fluid flow because initially highly fractured steps are important conduits whereas the fault core developed later on could act as a barrier for fluids when characterized by very low cross-fault permeability (AYDIN, 2000; FLODIN *et al.*, 2005). Second, being able to predict the architecture of large strike-slip faults with resolvable slip magnitude could provide insights into the distribution and characteristics of associated secondary faults, which

may not be detected by seismic techniques if they accommodate small magnitudes of slip. These secondary faults could develop as splays associated with the tip regions of the main fault segments (FLODIN and AYDIN, 2004; DE JOUSSINEAU and AYDIN, 2007; Fig. 1c), and may have length and angular properties correlated with the length of and spacing between segments composing the strike-slip fault systems (DE JOUSSINEAU *et al.*, 2007). Thus evaluating the number of segments composing the main strike-slip fault along with their length and spacing (given by the step width) could provide ways of estimating the location, frequency, and length and angular properties of the associated secondary faults. The prediction of such secondary faults is critical because they strongly influence the geometrical and statistical properties of damage zones (DE JOUSSINEAU and AYDIN, 2007). They could also enhance fracture connectivity by linking distant faults (as in Fig. 1c), and may increase the compartmentalization of the medium when they have a continuous core with low permeability.

5. Conclusions

We have provided new data for the remarkable self-similar architecture of strike-slip fault systems from the Valley of Fire State Park (SE Nevada), in addition to published data sets and maps. The new data set collected from the same region and rock type complements the published data and interpretations and lends support for the previous results related to the general trends in fault scaling. First, we have determined that the number of fault steps (hence fault segments) per unit length is correlated to the maximum fault offset by a negative power law over five orders of magnitude of the offset, suggesting that fault traces become progressively smoother with increasing offset. Second, we have determined that the mean segment length, mean step length and mean step width are all correlated to the maximum fault offset by positive power laws. In addition, we have analyzed the segment length distributions in four of the faults with offsets ranging from 80 m to 100 km. These distributions are similar in such that they are all lognormal, with most of the fault segments with a length in the interval of one to five times the fault offset. Finally, the steps composing the strike-slip fault systems have an approximately constant length-to-width ratio. These results are consistent with the commonly accepted concepts that strike-slip fault trace geometries become smoother and simpler as their offsets increase.

These fault scaling relationships usually have slightly different trends for the data sets from the Valley of Fire State Park, Nevada, our detailed study area, and the data sets from other geographic and geological environments. These differences, as proposed by the earlier investigators, could be due to the types and rheology of rocks, geological environments, and the fault growth processes. It is also possible that the scale of observation may cause artifacts in the fault scaling relationships.

These conclusions shed light onto the processes involved in the growth of natural faults over a broad range of scales. The data sets may be used as tools to better

characterize the architecture of subsurface strike-slip fault systems and to estimate useful parameters for subsurface applications, with critical implications for earthquake ruptures and fluid flow in the Earth's crust.

Acknowledgements

We acknowledge support from the Department of Energy, Basic Energy Sciences, Geosciences Research Program (Grant # DE-FG03-94ER14462 to Atilla Aydin and David D. Pollard). We thank the Valley of Fire State Park Rangers for permission to work in some areas of the Park where regular visitors are not allowed, and Ann-Laure Moreau for providing assistance in the field. Finally, we acknowledge the comments and suggestions by Yehuda Ben Zion, Mike Oskin and an anonymous reviewer.

REFERENCES

- AKI, K. (1989), *Geometric features of a fault zone related to the nucleation and termination of an earthquake rupture*. In Proc. Conf. XLV *Fault Segmentation and Controls of Rupture Initiation and Termination*, U.S. Geological Survey Open-File Report 89-315, 1-9.
- AYDIN, A. (2000), *Fractures, faults, and hydrocarbon entrapment, migration and flow*, Marine Petrol. Geol. 17, 797-814.
- AYDIN, A. and SCHULTZ, R.A. (1990), *Effect of mechanical interaction on the development of strike-slip faults with echelon patterns*, J. Struct. Geol. 12, 123-129.
- AYDIN, A. and NUR, A. (1982), *Evolution of pull-apart basins and their scale independence*, Tectonics 1, 91-105.
- BARKA, A. and KADINSKY-CADE, K. (1988), *Strike-slip fault geometry in Turkey and its influence on earthquake activity*, Tectonics 7, 663-684.
- BEN-ZION, Y. and SAMMIS, C.G. (2003), *Characterization of fault zones*, Pure Appl. Geophys. 160, 677-715.
- BOUCHON, M., CAMPILLO, M., and COTTON, F. (1998), *Stress field associated with the rupture of the 1992 Landers, California, earthquake and its implications concerning the fault strength at the onset of the earthquake*, J. Geophys. Res. 103, 21091-21097.
- BRANKMAN, C.M. and AYDIN, A. (2004), *Uplift and contractional deformation along a segmented strike-slip fault system: The Gargano Promontory, southern Italy*. J. Struct. Geol. 26, 807-824.
- CAINE, J.S., EVANS, J.P., and FORSTER, C.B. (1996), *Fault zone architecture and permeability structure*, Geology 24, 1025-1028.
- CARTWRIGHT, J.A., TRUDGILL, B.D., and MANSFIELD, C.S. (1995), *Fault growth by segment linkage: An explanation for scatter in maximum displacement and trace length data from the Canyonlands Grabens of SE Utah*, J. Struct. Geol. 17, 1319-1326.
- CEMBRANO, J., GONZÁLEZ, G., ARANCIBIA, G., AHUMADA, I., OLIVARES, V., and HERRERA, V. (2005), *Fault zone development and strain partitioning in an extensional strike-slip duplex: A case study from the Mesozoic Atacama fault system, Northern Chile*, Tectonophysics 400, 105-125.
- COWIE, P.A. and SCHOLZ, C.H. (1992a), *Displacement-length scaling relationship for faults: Data synthesis and discussion*, J. Struct. Geol. 14, 1149-1156.
- DAWERS, N.H., ANDERS, M.H., and SCHOLZ, C.H. (1993), *Growth of normal faults: Displacement-length scaling*, Geology 21, 1107-1110.
- DE JOUSSINEAU, G. and AYDIN, A. (2007), *The evolution of the damage zone with fault growth and its multiscale characterization*, J. Geophys. Res. 112, B12401, doi:10.1029/2006JB004711.

- DE JOUSSINEAU, G., MUTLU, O., AYDIN, A., and POLLARD, D.D. (2007), *Characterization of strike-slip fault-splay relationships in sandstone*, J. Struct. Geol. 29, 1831–1842.
- EICHHUBL, P., TAYLOR, W.L., POLLARD, D.D., and AYDIN, A. (2004), *Paleo-fluid flow and deformation in the Aztec Sandstone at the Valley of Fire, Nevada—Evidence for the coupling of hydrogeologic, diagenetic and tectonic processes*, Geol. Soc. Am. Bull. 116, 1120–1136.
- FINZI, Y., HEARN, E.H., BEN-ZION, Y., and LYAKHOVSKY, V. (2009), *Structural properties and deformation patterns of evolving strike-slip faults: Numerical simulations incorporating damage rheology*, Pure Appl. Geophys., in press.
- FLODIN, E., and AYDIN, A. (2004), *Evolution of a strike-slip fault network, Valley of Fire State Park, southern Nevada*, Geol. Soc. Am. Bull. 116, 42–59.
- FLODIN, E.A., GERDES, M., AYDIN, A., and WIGGINS, W. D. (2005), *Petrophysical properties of cataclastic fault rock in sandstone*. In *Faults, Fluid Flow, and Petroleum Traps* (eds. Sorkhabi, R., and Tsuji, Y.) American Association of Petroleum Geologists Memoir 85, 197–227.
- FU, B. and AWATA, Y. (2006), *Displacement and timing of left-lateral faulting in the Kunlun Fault Zone, northern Tibet, inferred from geologic and geomorphic features*, J. Asian Earth Sci. 29, 253–265.
- HARRIS, R.A., ARCHULETA, R.J., and DAY, S. M. (1991), *Fault steps and the dynamic rupture process: 2-d simulation of a spontaneously propagating shear fractures*, Geophys. Res. Lett. 18, 893–896.
- HARRIS, R.A. and DAY, S.M. (1999), *Dynamic 3D simulation of earthquakes on en echelon faults*, Geophys. Res. Lett. 26, 2089–2092.
- JACHENS, R.C., LANGENHEIM, V.E., and MATTI, J.C. (2002), *Relationship of the 1999 Hector Mine and 1992 Landers fault ruptures to offsets on Neogene faults and distribution of late Cenozoic basins in the Eastern California Shear Zone*, Bull. Seismol. Soc. Am. 92, 1592–1605.
- JOURDE, H., FLODIN, E.A., AYDIN, A., and DURLONSKY, L.J. (2002), *Computing permeability of fault zones in eolian sandstone from outcrops measurements*, Am. Assoc. Petrol. Geologists Bull. 86, 1187–1200.
- KIM, Y., PEACOCK, D.C.P., and SANDERSON, D.J. (2004), *Fault damage zones*, J. Struct. Geol. 26, 503–517.
- KNOTT, S.D., BEACH, A., BROCKBANK, P.J., LAWSON BROWN, J., MCCALLUM, J.E., and WELBON, A.I. (1996), *Spatial and mechanical controls on normal fault populations*, J. Struct. Geol. 18, 359–2372.
- LANGENHEIM, V.E., GROW, J.A., JACHENS, R.C., DIXON, G.L., and MILLER, J.J. (2001), *Geophysical constraints on the location and geometry of the Las Vegas Valley Shear Zone, Nevada*, Tectonics 20, 189–209.
- LAWRENCE, R.D., HASAN KHAN, S., and NAKATA, T. (1992), *Chaman Fault, Pakistan-Afghanistan*, Annales Tectonicae 6, 196–223.
- LE PICHON, X., ŞENGÖR, A.M.C., DEMIRBAĞ, E., RANGIN, C., İMREN, C., ARMİJO, R., GÖRÜR, N., ÇAĞATAY, N., MERCIER DE LEPINAY, B., MEYER, B., SAATÇILAR, R., and TOK, B. (2001), *The active Main Marmara Fault*, Earth Planet. Sci. Lett. 192, 595–616.
- MARUYAMA, T. and LIN, A. (2002), *Active strike-slip faulting history inferred from offsets of topographic features and basement rocks: A case study of the Arima-Takatsuki Tectonic line, southwest Japan*, Tectonophysics 344, 81–101.
- MYERS, R. and AYDIN, A. (2004), *The evolution of faults formed by shearing across joint zones in sandstone*, J. Struct. Geol. 26, 947–966.
- NEMER, T. and MEGHRAOUI, M. (2006), *Evidence of coseismic ruptures along the Roum fault (Lebanon): A possible source for the AD 1837 earthquake*, J. Struct. Geol. 28, 1483–1495.
- ODLING, N.E., HARRIS, S.D., and KNIPE, R.J. (2004), *Permeability scaling properties of fault damage zones in siliclastic rocks*, J. Struct. Geol. 26, 1727–1747.
- OTSUKI, K. and DILOV, T. (2005), *Evolution of self-similar geometry of experimental fault zones; implications for seismic nucleation and earthquake size*, J. Geophys. Res. 110, B03303, doi:10.1029/2004JB003359.
- PACHELL, M.A. and EVANS, J.P. (2002), *Growth, linkage, and termination processes of a 10-km-long strike-slip fault in jointed granite: The Gemini fault zone, Sierra Nevada, California*, J. Struct. Geol. 24, 1903–1924.
- POLLARD, D.D. and SEGALL, P., *Theoretical displacement and stresses near fractures in rock: With applications to faults, joints, veins, dikes, and solution surfaces*. In *Fracture Mechanics of Rock* (ed. Atkinson, B.K.) (Academic Press 1987) pp 277–349.
- RHODES, B.P., PEREZ, R., LAMJUAN, A., and KOSUWAN, S. (2004), *Kinematics and tectonic implications of the Mae Kuang Fault, northern Thailand*, J. Asian Earth Sci. 24, 79–89.
- ROVIDA, A., and TIBALDI, A. (2005), *Propagation of strike-slip faults across Holocene volcano-sedimentary deposits, Pasto, Colombia*, J. Struct. Geol. 27, 1838–1855.

- SCHLISCHE, R.W., YOUNG, S.S., ACKERMANN, R.V., and GUPTA, A. (1996), *Geometry and scaling relations of a population of very small rift-related normal faults*, *Geology* 24, 683–686.
- SCHOLZ, C.H., *The Mechanics of Earthquakes and Faulting*, 2nd revised edition (Cambridge University Press 2002).
- SEGALL, P. and POLLARD, D.D. (1980), *Mechanics of discontinuous faults*, *J. Geophys. Res.* 85, 4337–4350.
- SHAW, B.E. and DIETERICH, J.H. (2007), *Probabilities for jumping fault segment stepovers*, *Geophys. Res. Lett.* 34, L01307, doi:[10.1029/2006GL027980](https://doi.org/10.1029/2006GL027980).
- SIBSON, R.H. (1985), *Stopping of earthquake ruptures at dilational fault jogs*, *Nature* 316, 248–251.
- SIBSON, R.H. (1986), *Rupture interaction with fault jogs*. In *Earthquake Source Mechanics* (eds. Das, S., Boatwright, J., and Scholz, C.H.) (Am. Geophys. Union 1986) pp. 157–167.
- SIEH, K. and NATAWIDJAJA, D. (2000), *Neotectonics of the Sumatran fault, Indonesia*, *J. Geophys. Res.* 105, 28295–28326.
- STIRLING, M.W., WESNOUSKY, S.G., and SHIMAZAKI, K. (1996), *Fault trace complexity, cumulative slip, and the shape of the magnitude-frequency distribution for strike-slip faults: A global survey*, *Geophys. J. Internat.* 124, 833–868.
- TATAR, O., PIPER, J.D.A., GÜRSOY, H., HEIMANN, A., and KOÇBULUT, F. (2004), *Neotectonic deformation in the transition zone between the Dead Sea Transform and the East Anatolian fault Zone, Southern Turkey: A palaeomagnetic study of the Karasu Rift Volcanism*, *Tectonophysics* 385, 17–43.
- WALKER, R. and JACKSON, J. (2002), *Offset and evolution of the Gowk fault, S.E. Iran: a major intra-continental strike-slip system*, *J. Struct. Geol.* 24, 1677–1698.
- WALKER, R.T., BAYASGALAN, A., CARSON, R., HAZLETT, R., MCCARTHY, L., MISCHLER, J., MOLOR, E., SARANTSETSEG, P., SMITH, L., TSOGTBADRAKH, B., and THOMPSON, G. (2006), *Geomorphology and structure of the Jid right-lateral strike-slip fault in the Mongolian Altay mountains*, *J. Struct. Geol.* 28, 1607–1622.
- WESNOUSKY, S.G. (1988), *Seismological and structural evolution of strike-slip faults*, *Nature* 335, 340–342.
- WESNOUSKY, S.G. (2006), *Predicting the endpoints of earthquake ruptures*, *Nature* 444, 358–360.

(Received August 26, 2008, accepted March 30, 2009)

Published Online First: July 29, 2009

To access this journal online:
www.birkhauser.ch/pageoph
